Eur Biophys J (2009) 38:245–254
DOI 10.1007/s00249-008-0376-y

ORIGINAL PAPER

Physical properties of the specific PapG–galabiose binding in *E. coli* P pili-mediated adhesion

Oscar Björnham · Håkan Nilsson · Magnus Andersson · Staffan Schedin

Received: 27 June 2008 / Revised: 19 September 2008 / Accepted: 23 September 2008 / Published online: 16 October 2008

Abstract Detailed analyses of the mechanisms that mediate binding of the uropathogenic *Escherichia coli* to host cells are essential, as attachment is a prerequisite for the subsequent infection process. We explore, by means of force measuring optical tweezers, the interaction between the galabiose receptor and the adhesin PapG expressed by P pili on single bacterial cells. Two variants of dynamic force spectroscopy were applied based on constant and non-linear loading force. The specific PapG–galabiose binding showed typical slip-bond behaviour in the force interval (30–100 pN) set by the pilus intrinsic biomechanical properties. Moreover, it was found that the bond has a thermodynamic off-rate and a bond length of 2.6×10^{-3} s^{-1} and 5.0 Å, respectively. Consequently, the PapG–galabiose complex is significantly stronger than the internal bonds in the P pilus structure that stabilizes the helical chain-like macromolecule. This finding suggests that the specific binding is strong enough to enable the P pili rod to unfold when subjected to strong shear forces in the urinary tract. The unfolding process of the P pili rod promotes the formation of strong multipili interaction, which is important for the bacterium to maintain attachment to the host cells.

Keywords *Escherichia coli* · Non-covalent single bond · Slip-bond · Dynamic force spectroscopy · Receptor–ligand interaction

O. Björnham · H. Nilsson · S. Schedin (✉)
Department of Applied Physics and Electronics,
Umeå University, 901 87 Umeå, Sweden
e-mail: staffan.schedin@tfe.umu.se

M. Andersson
Department of Physics, Umeå University, 901 87 Umeå, Sweden

Abbreviations

UPEC	Uropathogenic *Escherichia coli*
UTI	Urinary tract infection
FMOT	Force measuring optical tweezers
AFM	Atomic force microscopy
DFS	Dynamic force spectroscopy
MSE	Mean square error

Introduction

Uropathogenic *Escherichia coli* (UPEC) is the major aetiological agent associated with urinary tract infection (UTI). UPEC is accountable for 80% of the community-acquired UTI infections (Foxman and Brown 2003), including pyelonephritis and cystitis (Reid and Sobel 1987; Sandberg et al. 1988). The first step in an infection is the adherence of bacteria to uroepithelium cells. *E. coli* demonstrates diverse properties at different environment, and can express a variety of attachment organelles (pili) on the outer membrane, which mediate adhesion to specific receptors on uroepithelial cells (Enami et al. 1999). Two types of pili, P and type 1 pili, are commonly associated with UPEC and with infections in the upper and the lower urinary tract, respectively. They have similar geometrical structure, but there are distinct differences in their biomechanical properties (Andersson et al. 2007). Both types express an adhesion molecule at the distal end of the pili; P pilus has the PapG adhesin whereas type 1 has the FimH adhesin (Weissman et al. 2006). The PapG adhesin forms specific bonds with the glycolipid galabiose (Larsson et al. 2003; Lund et al. 1987; Ohlsson et al. 2002; Stromberg et al. 1990) and the FimH binds specifically to mannose (Forero et al. 2004; Nilsson et al. 2006; Thomas et al. 2006; Thomas et al. 2004).

Specific adhesin–receptor bonds normally behave as slip-bonds when they are subjected to an external force. A slip-bond is defined as a bond whose life-time is shortened by an external force that lowers the energy barrier between the bound and the free state, and the bond can thereby dissociate more easily (Bell 1978). However, counter-intuitively, an external force can also prolong the life-time of a bond (increase the binding strength). The existence of this catch-bond behaviour was first suggested by Dembo et al. (1988) with the hypothesis that the external force deformed the binding molecules such that they locked more tightly. More recently, several theories have been proposed to model the catch-bond behaviour observed in different binding complexes (Evans et al. 2004; Guo and Guilford 2006; Thomas et al. 2006). Moreover, a bond whose life-time is independent of external forces is referred to as an ideal bond and can be regarded as the limit between a slip-bond and a catch-bond. The type 1 pilus has been found to possess a catch-bond mechanism through the specific FimH-mannose binding (Thomas et al. 2002). The catch-bond mechanism allows the bacteria to stay bound to a surface during a temporarily increased shear flow in its surrounding. This property could be essential for the bacterium to prevent being rinsed out from the urinary tract system and still be able to unbind occasionally, when no shear force is present. To some extent Nilsson et al. (2006) showed that the P pilus also expresses a catch-bond property when bonded to digalactose, in a limited shear force interval, using the stick-and-roll approach.

Bacterial pili have previously been characterised by means of force measuring optical tweezers (FMOT) and atomic force microscopy (AFM) (Jass et al. 2004; Liang et al. 2000; Maier et al. 2002; Miller et al. 2006). Lugmaier et al. (2007) studied the specific PapG–galabiose binding by means of AFM and assessed both the bond length and the thermal off-rate. In contrast to that work, we probe the specific PapG–galabiose bond by FMOT at different loading conditions set by the intrinsic force-elongation properties of the biopolymer. Initially, the pilus is linearly elongated as a mechanical spring when it is exposed to a tensile force (region I). Next, the force-elongation response turns into a phase of constant force as the pilus undergoes a sequential unfolding process where the quaternary helical structure is transformed into a linear structure (region II). If the tension is further increased, the pilus responds with non-linear force-elongation dependence (region III). The complex force response under tensile stress has previously been investigated (Jass et al. 2004).

In this study, we used FMOT to assess the PapG–galabiose off-rate and bond length by means of dynamic force spectroscopy (DFS). The analysis is based on measured unbinding forces, collected during the constant force plateau (region II) and the non-linear response (region III). In addition, we model the force-elongation of a complete pilus, including the specific PapG–galabiose interaction, with a three-state Monte Carlo simulation. The above mentioned methods, allowed us to assess the bond length and thermodynamic off-rate with high accuracy, but also to conclude whether the specific interaction can be described as a slip-bond or as a catch-bond.

Materials and methods

Measurements were performed with a FMOT system constructed around an inverted Olympus IX71 microscope with a high numerical aperture objective. A detailed description of the optical tweezers and the calibration procedure is given elsewhere (Andersson et al. 2006a; Fällman et al. 2004). Force measurements were conducted at three different velocities; 0.5, 5.0 and 50 μm/s. In total, we performed 720 measurements, distributed at the three mentioned velocities. In addition, 120 negative control measurements were conducted.

General experimental procedure

The amino-galabiose was covalently coupled to activated 3.2 μm carboxymethyl latex beads (Interfacial Dynamics Corp, Portland, Oregon, USA). A 30 μl suspension of viable bacteria expressing P pili and free floating amino-galabiose coated latex beads was prepared between two coverslips. Large 9.6 μm beads were fixed to the surface of the lower coverslip by means of drying at 60°C for 60 min. Poly-L-Lysine (Sigma–Aldrich, Stockholm, Sweden) was coupled to the large beads in order to provide an adhesive surface for attachment of single bacterial cells. This binding is substantially stronger than the receptor–ligand binding which ensures that the bacterium does not unbind during experiments. Initially in the experiment, one bacterium was trapped with the optical tweezers and mounted to a fixed large bead. Moreover, a 3.2 μm bead was subsequently trapped and brought to close proximity to the mounted bacterium to form a specific binding between a single PapG adhesin (at the distal end of a pilus) and the galabiose receptor molecule. The coverslip, with the large bead and the mounted bacterium, was retracted from the trapped bead using a piezo stage. The resulting force-elongation response of the pilus was probed and recorded until the binding ruptured. The qualitative force-elongation response for a single P pilus has been determined previously (Jass et al. 2004). The constant force plateau in region II is very distinct and easy to identify. Thus, we can determine the number of attached pili and filter out multipili attachment from the force level of the plateau.

Bacterial strains

A derivative of the fully afimbriated *E. coli* K12 strain HB101 was utilised in order to ensure solely P pili expression. The strain HB101/pPAP5 expresses P pili via a complete pap gene cluster that has been cloned into a pBR322 vector, thereby creating plasmid pPAP5 (Lindberg et al. 1987; Lindberg et al. 1984). The HB101/pPAP5 was grown at 37°C on trypticase soy agar that was enriched with 50 μg/ml carbenicillin.

Negative control

Negative control measurements were conducted to ensure the specificity of the PapG–galabiose binding. In order to block the PapG adhesins, solution galabiose was added to the medium, resulting in a concentration of 3 mM. These measurements were in all other aspects conducted at identical conditions as the unbinding measurements. Bindings to P pili were detected only at 2.5% of the measurements. This should be compared to the case without the galabiose solvent, where binding occurred in almost every measurement. The significantly reduced binding probability, when the adhesins were blocked, confirmed the specificity of the measurements.

Theory

The biomechanical properties of the P pilus structure have been thoroughly investigated previously (Andersson et al. 2006a; Björnham et al. 2008; Jass et al. 2004). The known pilus properties were used as a foundation for further analysis and evaluation methods of the specific PapG–galabiose bond. Moreover, specific results were acquired in several ways using quantitative facts of the pilus properties. The P pilus force response can, with advantage, be divided into three regions, see Fig. 1a.

The various characteristics of the force-elongation response of a single P pilus provide diverse loading conditions when probing the unbinding forces of the PapG–galabiose bond. There is a constant force ramp (linearly increasing force-elongation relation) in region I, which would allow for DFS with a constant loading rate using the well known theory established by Evans et al. (Bell 1978; Evans 2001; Evans and Ritchie 1997). However, in our case, this would be very time consuming since the pilus enters region II already at steady-state level ∼28 pN, which indicates that experiments would have to be performed under extremely low loading rates to be able to probe the most likely rupture force below the steady-state force level. In region II, the pilus is unfolding (the helical quaternary structure transforms into a linear structure) and responds with constant force-elongation dependence. This allows for measurements of the constant off-rate as long as a significant fraction of the PapG–galabiose binding measurements rupture in this region. Finally, in region III, the pilus exhibits a complicated force-elongation response that can be used for non-linear DFS analysis since the shape of the force response is known (Andersson et al. 2006c). The analysis methods for regions II and III are described in detail below.

Region II—DFS with a constant loading force

It has been shown by Jass et al. (2004) that the force response in region II is a constant force plateau. The force-elongation is in steady-state for velocities up to ∼0.4 μm/s, i.e. the force response is velocity-independent. Above that, it enters a dynamic regime where the magnitude of the constant force plateau depends linearly on the logarithm of the velocity (Andersson et al. 2006a). A constant force-elongation response implies a constant off-rate, i.e. for different velocities the off-rates take dissimilar values but, in each individual case, remains constant over the entire region. For a constant off-rate, k_{off}, the probability, p, for a

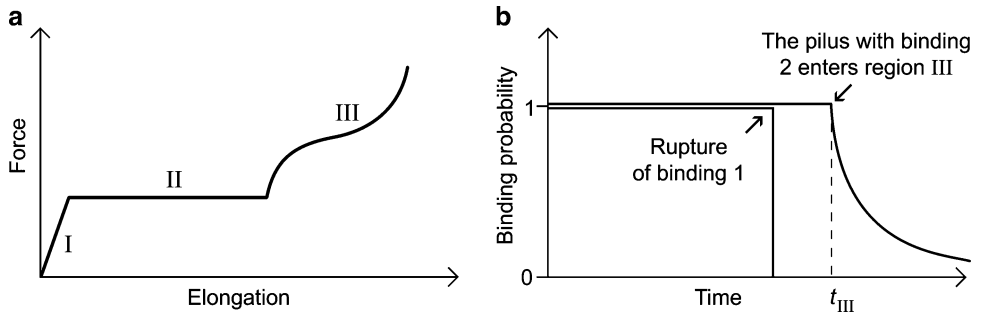

Fig. 1 **a** A schematic diagram of a force-elongation response of a P pilus where the three regions are defined. **b** Illustration of the probability analysis principle for two different binding procedures. In the first case, the binding ruptures in region II and its probability contribution is described by a step-function. In the second case, the pilus enters region III, at time t_{III}, and the probability contribution from the binding is from that point described by an exponentially decreasing function

bond, that is bound at $t = 0$, to survive is described by an exponentially decreasing function with time, t, is

$$p = \mathrm{e}^{-k_{\mathrm{off}}t}. \quad (1)$$

If the expected time of survival, k_{off}^{-1}, is small compared to the time spent in region II, virtually all bonds will rupture in region II, and k_{off} can be retrieved by a direct fit of the theoretical $p(t)$ to the measured data. However, the fraction of rupture events in region II is only between 30 and 50% in our measurements. Further, since the pili are of different length, those that survive region II enter region III at dissimilar distances. A more advanced fitting method is therefore needed to include the data for the pili that enters region III into the analysis. For those pili we modelled the binding probability as if the force had remained at the same constant level after they have entered region III. The theory of bond kinetics used in this work assumes no memory in the system, i.e. the kinetic probability functions for time $t \geq t_{\mathrm{a}}$ (where t_{a} is an arbitrary time) depends only on state parameters, not on the history at time $t < t_{\mathrm{a}}$. This implies that a bond that survives until it enters region III at time, t_{III}, would have the probability function $p = \exp(-k_{\mathrm{off}}(t - t_{\mathrm{III}}))$for $t \geq t_{\mathrm{III}}$ if the force had remained constant, since it is known to satisfy $p(t = t_{\mathrm{III}}) = 1$. This procedure was implemented in the analysis by replacing the probability contribution from a pilus that enters region III (at time t_{III}) with an exponentially decreasing probability function for $t \geq t_{\mathrm{III}}$, see Fig. 1b. The off-rate, k_{off}, is required to introduce the probability function for $t \geq t_{\mathrm{III}}$. Since this parameter is unknown and will be determined by a fit to the measured data, we have an implicit relation. The measured data includes k_{off} for all measurements that enters region III. This set of data is at the same time the basis for a fit using Eq. 1, which also includes k_{off}. A range of different attempt values of k_{off} were used in a series of fits where the best fit supplied the off-rate.

Further on, the data from region II provides an excellent opportunity to investigate whether the PapG–galabiose complex is a slip-bond or a catch-bond. For a given velocity, the force, and thereby the off-rate, is constant in region II which implies that the bond can be classified from measurements performed at different velocities. For a slip-bond, Bell postulated that the off-rate of a molecular bond is exponentially dependent on the applied force, f, which here is formulated as

$$k_{\mathrm{off}} = k_{\mathrm{off}}^{\mathrm{th}} e^{\frac{fx_{\mathrm{b}}}{k_{\mathrm{B}}T}}, \quad (2)$$

where $k_{\mathrm{off}}^{\mathrm{th}}$ is the thermal (spontaneous) off-rate, x_{b} is the bond length, k_{B} is the Boltzmann's constant and T is the absolute temperature (Bell 1978). This implies that the slope in a diagram of $\ln(k_{\mathrm{off}})$ versus f yields the bond length,

$$\Delta \ln(k_{\mathrm{off}})/\Delta f = x_{\mathrm{b}}/k_{\mathrm{B}}T. \quad (3)$$

The thermal off-rate can be derived from the intersection between the linear fit and the vertical axis where the force is equal to zero.

Region III—DFS with a non-linear loading force

The force-elongation response in region III is in steady-state within the range of velocities used here (Andersson et al. 2006a), and thereby independent of the velocity. However, there are two factors that differentiate the probabilities of rupture forces in region III for different velocities. First, the point of entry into region III depends on the constant force level in region II, and thereby of the velocity. Second, higher velocities will probe region III faster which means that the loading rate increases with the velocity. DFS applied to slip-bonds is normally conducted using a linear force ramp as loading condition. The theory for analysis is well established (Bell 1978; Evans 2001; Evans and Ritchie 1997) and has been implemented in a variety of biological systems (Morfill et al. 2007; Odorico et al. 2007; Yang et al. 2007). However, since the force profile of region III is highly non-linear, this theory has limited applicability under such conditions. For this reason, we present a more general form of the theory that can be used for an arbitrary loading force that is continuous with a low second derivative with respect to time.

The change in binding probability can in general, with no rebinding, be written as

$$\mathrm{d}p/\mathrm{d}t = -k_{\mathrm{off}}p. \quad (4)$$

Moreover, at the time where the rupture probability has a maximum, the requirement

$$\mathrm{d}k_{\mathrm{off}}/\mathrm{d}t = k_{\mathrm{off}}^2, \quad (5)$$

applies. This point of time can be identified by localising the maximum of a rupture force distribution histogram. Equation 5 can be derived by differentiating Eq. 4, with respect to time, and identifying the point of maximum rupture probability. The off-rate function can be expressed as

$$k_{\mathrm{off}} = k_{\mathrm{off}}^{\mathrm{th}} \mathrm{e}^{Bx_{\mathrm{b}}}, \quad (6)$$

where B is a function that describes the time evolution of the force as

$$B \equiv f/k_{\mathrm{B}}T. \quad (7)$$

Using Eq. 6, the first derivate of the off-rate with respect to time is

$$dk_{off}/dt = k_{off} x_b dB/dt, \quad (8)$$

and inserting this into Eq. 5 yields

$$k_{off} = x_b dB/dt = x_b A, \quad (9)$$

where we introduce $A \equiv dB/dt$ for simplicity reason. Equations 6 and 9 results in an expression for the thermal off-rate,

$$k_{off}^{th} = A x_b e^{-B x_b}. \quad (10)$$

This relation only applies at the time of the most probable rupture force, i.e. the most probable rupture time. To conclude this derivation we take the logarithm of both sides of Eq. 10,

$$\ln\left(k_{off}^{th}/x_b\right) - \ln(A) = -B x_b. \quad (11)$$

Note that the first term on the left hand side is a constant and the slope of $\ln(A)$ versus B equals x_b. Further on, the thermal off-rate k_{off}^{th} is given by $k_{off}^{th} = A x_b$ where $B = 0$ on the extrapolated linear fit.

Monte Carlo simulation

A third method to extract the thermal off-rate and bond length for the PapG–galabiose complex is by simulating and fitting the experimental data by a three-state Monte Carlo method. We used the same approach as described by Björnham et al. (2008), with the introduction of an additional function that models the binding of the PapG-adhesion to the galabiose receptor in order to calculate the rupture probability. All other parameters were set to the same values as presented in (Björnham et al. 2008) which generates the force-elongation response of a typically P pilus. The probability profile could then be compared to the measured data for different sets of the parameters k_{off}^{th} and x_b in search for the best fit.

Results and discussion

The measurement data were analysed by three different methods, where the first two are categorised as DFS methods. The first one is based on the set of unbinding probabilities collected during the constant force-elongation plateau (region II). The second method analyzes the unbinding forces during the non-linear force-elongation response (region III). Finally, in the third method we applied Monte Carlo simulations to fit all data, i.e. data from both regions are analysed simultaneously.

Histograms of the measured rupture probability distributions at the three different velocities (0.5, 5.0 and 50 μm/s) are presented in Fig. 2a. We clearly observe the dynamic behaviour of the force response, i.e. the force distributions are shifted towards higher forces as the velocity increases. The distributions plotted in Fig. 2a have two relevant local maxima. The maxima in the low force interval originates from the rupture events measured during the constant force plateau (region II), whereas the one in the high interval is generated from the rupture events in region III. In the former case, the mean of the force levels were 32, 45 and 63 pN for the velocities 0.5, 5.0 and 50 μm/s, respectively. The first peak in each histogram corresponds to these force values. Moreover, nearly no binding (97.5% rupture probability at zero force) could be detected for the negative control measurements with solution galabiose.

Region II—DFS with a constant loading force

The constant force plateau, region II, is typically ~5 μm long; however, it can vary within a few μm between individual pili (Andersson et al. 2006c). Moreover, the time at which the system is found in region II is directly

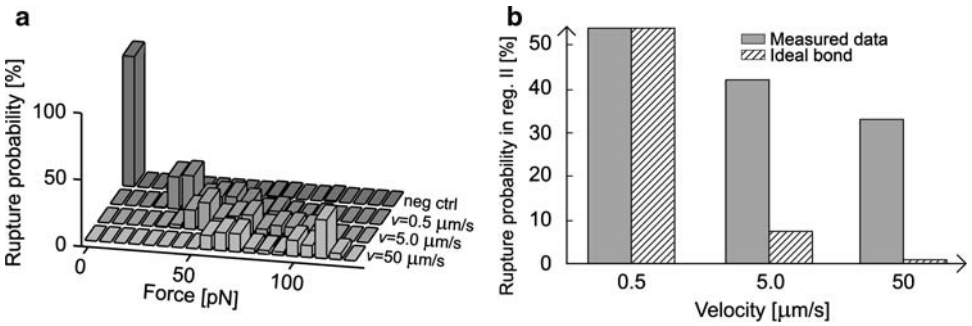

Fig. 2 **a** The measured rupture probabilities as a function of force for the velocities 0.5, 5.0 and 50 μm/s, respectively. The negative control measurements clearly demonstrate the specificity of the measurements. As the velocity increases, the rupture force distributions are shifted towards higher forces. This is the result of the amplified force-level in region II as well as the strongly increased loading rate in region III. The mean of the force levels were 32, 45 and 63 pN for the velocities 0.5, 5.0 and 50 μm/s, respectively. These values can also be recognised in the figure as the first peak in each histogram. **b** The total measured rupture probability in region II in comparison with that of an ideal bond. Here, the ideal bond is set to give rise to the same rupture probability as the measured one at the lowest speed. The measured rupture probabilities strongly deviate from the case with an ideal bond for the velocities 5.0 and 50 μm/s. For a catch-bond, these probabilities are expected to be even lower than that for the ideal bond for these velocities (i.e. higher forces). The conclusion is therefore that the specific PapG–galabiose bond is a slip-bond in the force interval treated here

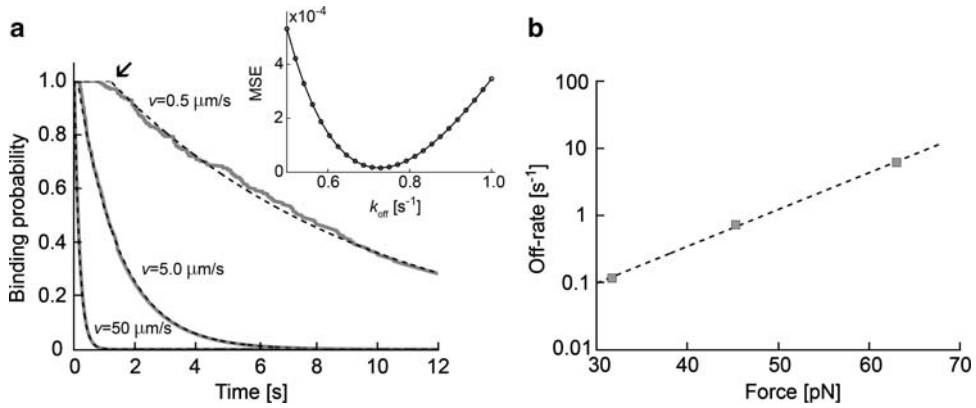

Fig. 3 **a** The thick grey line represents the measured binding probability, including the modelled contribution for the pili that entered region III, whereas the overlaid *dashed black line* is the best numerical fit. The *arrow* indicates the instant at which the unfolding length is 600 nm for the velocity of 0.5 μm/s. The *inset* shows the mean square error (MSE) for a range of off-rates for the velocity 5.0 μm/s. The minimum value corresponds to the best fit. The total number of measurements (with the number that ruptured in region II in parenthesis) was 176 (95), 239 (100) and 305 (101) for the velocities 0.5, 5.0 and 50 μm, respectively. **b** The three off-rates are plotted logarithmically versus their corresponding constant force levels. The bond length was derived from the slope of the fit and is 5.2 ± 0.3 Å. The extrapolated intersection with the vertical axis, at the point of zero force, supplied the thermal off-rate as $2.2 \times 10^{-3} \pm 0.9 \times 10^{-3}$ s^{-1}. The bond is classified as a slip-bond in this force interval since the off-rate increases with the applied force. The errors refer to the 95% confidence interval obtained by error analysis of exponential functions of the lifetimes followed by error propagation through the fitting procedure

proportional to the inverse of the trap velocity. This implies that at a velocity of 0.5 μm/s, the specific binding for a certain pilus has a tenfold longer time to dissociate, compared to the case with a velocity of 5.0 μm/s. As mentioned above, a result of the subunit assembled helix-like structure results in a dynamic force response which depends on the logarithm of the unfolding velocity (Andersson et al. 2006a). Therefore, the force level is significantly higher at 5.0 μm/s (45 pN) than at 0.5 μm/s (32 pN), which has an impact on the off-rate of the binding. It was found, as displayed in Fig. 2b, that the rupture probability for the bonds in region II was 54.0, 42.2 and 33.1% at the velocities 0.5, 5.0, and 50 μm/s, respectively. This change in unbinding frequency is moderate when considering the significant difference in exposure time in region II. Let us consider a hypothetical case with an ideal bond in region II, i.e. a bond with an off-rate that is independent of the force. We assign the ideal bond the same rupture probability as the measured one at 0.5 μm/s. If we evaluate the rupture probabilities at 5.0 and 50 μm/s for the ideal bond, using Eq. 1, the result is that they are drastically reduced due to the shorter time until the pilus enters region III, see Fig. 2b. It is evident that the measured data strongly deviate from the case with an ideal bond. The rupture probability would be even lower for a catch-bond than for an ideal bond when the force (i.e. the velocity) increases. The conclusion is therefore that the specific PapG–galabiose bond behaves as a typical a slip-bond in the force interval treated in this study.

To ensure that the force-elongation had entered region II, only measurements with a constant unfolding longer than 600 nm were analysed. Therefore, the numerical fit was adjusted so that the binding probability started to decrease when this elongation was reached, which is marked, for the 0.5 μm/s velocity data, with an arrow in Fig. 3a. As the PapG–galabiose bond is assumed to be history independent, similar to the pilus rod (Andersson et al. 2006b), the exclusion of the short-plateau data does not affect the extraction of the off-rate from the data. The measured binding probability presented in Fig. 3a includes both rupture events and the contribution from the measurements where the pili enter region III as described earlier.

Since our measurements were conducted at three velocities (0.5, 5.0 and 50 μm/s) we could assess three dissimilar off-rates for the PapG–galabiose bond (Fig. 3b), each corresponding to a constant force-level in region II. These three off-rates differ as a result of the exponential impact the force has on the off-rate, weighted by the bond length and the thermodynamic energy unit k_BT, see Eq. 2. The bond length, given by the slope of the linear fit of the logarithmic off-rate dependence on the force (the dashed line in Fig. 3b), is found to be $x_b = 5.2 \pm 0.3$ Å. The thermodynamic off-rate is derived by the extrapolation of the linear fit and amounts to $k_{off}^{th} = 2.2 \times 10^{-3} \pm 0.9 \times 10^{-3}$ s^{-1}.

Region III—DFS with a non-linear loading force

The optical tweezers system used in this work has a capability to measure forces up to ~100 pN with high accuracy. Above that, the optical trap is non-linear for these particular experiments. Although the force increases

rapidly with the elongation in region III, the upper limit of 100 pN was high enough for detection of nearly all of the unbinding forces for the two lowest retracting velocities (0.5 and 5.0 μm/s). In contrast, for the highest velocity (50 μm/s) the unbinding forces frequently exceeded 100 pN. This caused a problem, since the accuracy of the probability distribution was reduced.

Following the theory presented for the non-linear behaviour of region III we plotted the logarithm of the parameter A, versus the parameter B and applied a linear fit to obtain the bond length and the thermal off-rate. Histograms of the measured rupture forces, which provide values for B, are shown in Fig. 2a. The explicit time dependence of the force-elongation response for a pilus of average length in region III was calculated. This allowed us to derive the most probable rupture time and scrutinise the values for A. The time dependence of the force-elongation in region III has been shown to be predictable (Andersson et al. 2006c) and only weakly dependent of the length of the pilus, which was obtained from the length of region II. The data and the linear fit are displayed in Fig. 4a. Note that the data from the highest velocity is also plotted, however, since the accuracy is reduced, it was excluded in the linear fit. The bond length and the thermal off-rate obtained from this analysis were calculated to be $x_b = 4.9 \pm 0.4$ Å and $k_{off}^{th} = 3 \times 10^{-3} \pm 1 \times 10^{-3}$ s^{-1}, respectively.

Monte Carlo—MSE minimisation

From previous work, it was concluded that an average P pilus of the strain used here (HB101/pPAP5) is composed of ~1,430 PapA-subunits, which corresponds to ~5 μm elongation in region II (Andersson et al. 2006c). A larger number of subunits results in a longer elongation, which implies that the time in region II is extended, thus the probability for a rupture event in region II increases. Hence, short pili have a larger probability to survive and enter region III before rupture. From the experimental data we observed that the actual mean number of subunits of pili entering region III was ~900. The simulations were modified to compensate for this phenomenon. Two different simulations were performed for every set of parameters; one with 1,430 subunits and one with 900 subunits. The rupture probability distribution of the data with 1,430 subunits was used in regions I and II, whereas the one with 900 subunits was used in region III. These two distributions were merged after a renormalization of the rupture probability for the region III data.

Simulations with a multitude of combinations of bond lengths and thermal off-rates were performed to find the set of parameters that best reproduced the experimental data. The best fit was defined where the mean square error (MSE) was found to be at minimum, which is illustrated in the inset of Fig. 4b for the intervals ($4.5 \leq x_b \leq 5.0$ Å) and ($1.5 \times 10^{-3} \leq k_{off}^{th} \leq 4.2 \times 10^{-3}$ s^{-1}). The bond length and thermal off-rate were found to be 4.8 ± 0.2 Å and $2.5 \times 10^{-3} \pm 0.5 \times 10^{-3}$ s^{-1}, respectively.

Summary of the results and concluding remarks

From the analysis of region II we conclude that the off-rate increases from ~0.1 to ~6 s^{-1} when the constant force

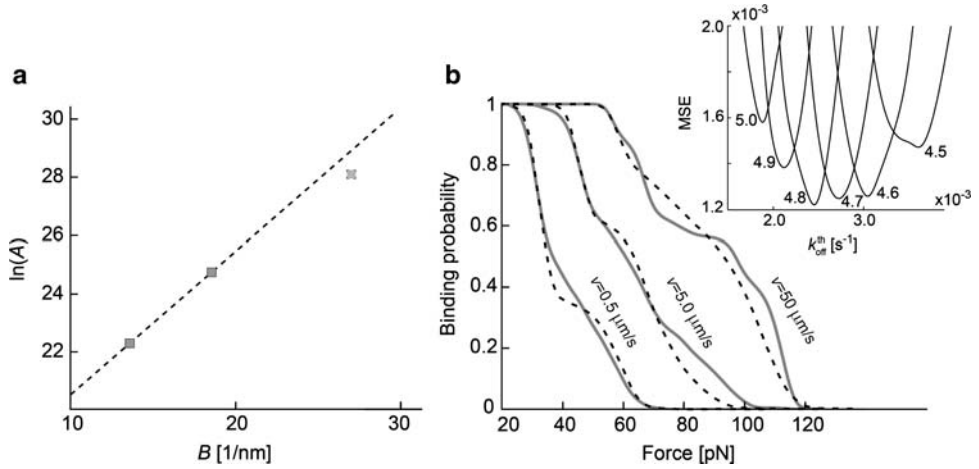

Fig. 4 **a** A linear fit of the rupture force modes of region III reveals both the bond length, 4.9 ± 0.4 Å, and the thermal off-rate, $3 \times 10^{-3} \pm 1 \times 10^{-3}$ s^{-1}. As some of the unbinding forces for the highest measurement velocity (50 μm/s) exceeded the linear limit of the measurement system, the results became unreliable and were therefore not used in the fit (the *dashed square*). **b** The binding probability profiles are illustrated for the measurements (*solid grey line*) and the Monte Carlo fits (*dashed black line*). The total number of measurements was 176, 239 and 305 for the velocities 0.5, 5.0 and 50 μm/s, respectively. The best fit was found for a bond length of 4.8 ± 0.2 Å and thermal off-rate of $2.5 \times 10^{-3} \pm 0.5 \times 10^{-3}$ s^{-1}. The *inset* shows the total variation of the mean square error (MSE), for all velocities, as a function of the thermal off-rate for a set of different bond lengths. The 95% confidence intervals were calculated from estimations of the maximum errors in the raw data processing and the following error propagation thereof

increases from 32 to 63 pN. This implies that the PapG–galabiose complex exhibits typical slip-bond behaviour in this force interval.

Thomas et al. (2006) showed that the specific FimH-mannose binding of type 1 pili can be classified as a catch-bond up to a certain breakpoint where the binding property converts into a slip-bond. This transient behaviour has also been reported for other systems (Barsegov and Thirumalai 2005; Evans et al. 2004). In addition, Nilsson et al. (2006) suggested the PapG–galabiose complex to is a catch-bond when tested at a shear–stress of $\leq$4.3 pN/μm^2 (by observing the number of tethered cells rolling on a surface at different shear–stresses). Goldman's approximation estimate the force acting on a spherical body under shear force when tethered to a wall (Goldman et al. 1967). In short, this approximation provides the drag force, F, on spherical object exposed to a shear flow according to

$$F = 1.7 \times 6\pi\mu rhS = 1.7 \times 6\pi rh\tau, \quad (12)$$

where μ is the viscosity of the fluid, r is the radius of the body, h is the distance between the wall and centre of the sphere, and S is the shear rate which can be related to the shear stress, τ, as $\tau = \mu S$. It is important to notice that there are pronounced differences between the ideal conditions in Goldman's approximation and a practical measurement with tethered bacteria. Issues such as the non-spherical shape of the bacterium, the relatively rough cell surface, presence of a multitude of pili, unknown orientation of the cell and biomolecules covering the wall surface may all contribute to an uncertainty of the calculated force using Goldman's approximation. Typical geometrical dimensions of an *E. coli* bacterium is $\sim$2 μm in width and $\sim$0.8 μm in diameter (Sundararaj et al. 2004). To use Goldman's approximation we calculated the effective radius of a sphere by mimicing the surface area of a typical bacterium. The drag force was computed with Eq. 12 to $\sim$40 pN at a shear rate of 4.3 pN/μm^2. This force is of similar order of magnitude as our measured forces. However, it is of great importance to recognise the differences between their model system and the one used in this work. Nilsson et al. (2006) performed stick-and-roll experiments where the bacteria are expected to interact with multiple bindings. The actual number of bindings in these types of measurements is unknown. However, as a bacterium normally expresses a rich amount of pili, it is reasonable to assume that numerous multiple bindings are present. The tensile force experienced in each individual binding (supported by each single pilus) can therefore be assumed to be significantly smaller than 40 pN, and is well below the force interval of the measured unbinding forces in this work. Since it is known that bonds can exhibit both slip and catch behaviour for different force intervals, it is essential to consider the force interval used in a study when the results are evaluated. For instance, it was first reported that selectins-ligand bonds were slip bonds (Evans et al. 2001; Fritz et al. 1998). Later it was concluded that these bonds also exhibit catch behaviour for lower forces (Evans et al. 2004; Marshall et al. 2003).

A binding system involving multipili attachments has inherently interesting binding properties. Let us assume that a loading force is unevenly distributed amongst the pili (e.g. one pilus is stretched and supports force whereas others are unstretched and do not support force). Initially, only one pilus supports force whilst more pili will support force after the first one has been elongated. A low unfolding rate (low force) can result in a rupture of the first pilus before the second one is exposed to force. At higher unfolding rate (higher force) the first pilus will elongate faster and the probability that its binding survives until the force is divided with the second binding can increase. The off-rate for each pilus will then decrease drastically since it depends exponentially on the applied force, see Eq. 2. This suggests that multipili attachments with slip-bonds can collectively exhibit apparent catch-bond behaviour, or at least moderate the true slip-bond behaviour. This phenomenon may be present in region II when the unfolding is in the dynamic regime. The analysis is therefore more complicated for multipili attachments than for the single pilus case. In conclusion, the collective properties of a multipili binding system cannot automatically be transferred to a single binding in that system.

There are two possible explanations for the contradictory conclusions regarding the slip- or catch-bond property between the present work and that reported by Nilsson et al. First, it is plausible that the catch-bond behaviour exists only in the low force interval which was exceeded for the applied forces (>32 pN) in the present work. Second, the apparent catch-bond behaviour reported by Nilsson et al. can be attributed to a multipili phenomenon rather than a catch-bond property of the individual PapG-galabiose bond.

From the same set of experimental data we assessed three pairs of bond lengths and thermal off-rates which are presented in Table 1. The average value from the three

Table 1 Summary of the parameters for the three different analysis methods. The error corresponds to a 95% confidence interval. The confidence intervals for the mean values were calculated using theory for sampling distributions

Method	x_b (Å)	k_{off}^{th} (s^{-1})
Region II	5.2 ± 0.3	0.0022 ± 0.0009
Region III	4.9 ± 0.4	0.003 ± 0.001
Monte Carlo	4.8 ± 0.2	0.0025 ± 0.0005
Mean	5.0 ± 0.2	0.0026 ± 0.0005

methods was used as estimates of the true values. This implies that the specific PapG–galabiose binding has a bond length of $x_b = 5.0 \pm 0.2$ Å and a thermal off-rate of $k_{off}^{th} = 2.6 \times 10^{-3} \pm 0.5 \times 10^{-3}$ s^{-1}.

Lugmaier et al. (2007) reported a bond length of 7.0 ± 1.5 Å and a thermal off-rate of $8.0 \times 10^{-4} \pm 5.0 \times 10^{-4}$ s^{-1} for the PapG-galabiose binding. Their measurement setup (model system) was similar to the one used here except for the fact that they used an AFM for probing the unbinding forces. The unbinding data was then fitted to a Monte Carlo model from which the parameter values were retrieved. The reason for the differences can be assumed to be a sum of three factors. First, FMOT has a higher force resolution than the AFM and thereby provides more precise data. Second, in this work we performed force measurements with three different velocities, in contrast to Lugmaier et al. where one single velocity (0.5 μm/s) was used. Finally, a larger statistical basis is used here, which is an important factor in a stochastic process such as a thermodynamic unbinding event.

Moreover, we conclude that the off-rate for the PapG–galabiose binding complex is several order of magnitudes lower than that for the layer-to-layer bond, which stabilize the quaternary helix-like structure of the folded pilus (Andersson et al. 2006a; Björnham et al. 2008). This finding confirms that the PapG–galabiose complex is sufficiently strong to withstand the forces required for unfolding the quaternary structure at physiological conditions. A similar observation is reported for the type 1 pilus when bound to monomannose (Forero et al. 2004). In an in vivo situation, it is likely that several pili, of dissimilar length and attachment positions, are involved simultaneously in the adhesion process. If a bacterium is exposed to a sudden shear force, e.g. due to urine flow, an uneven distribution of the force amongst the pili is expected. Initially, some pili (e.g. the shortest ones) are stretched and exposed to tension force. Other pili (e.g. the long ones), remain unstretched and will thereby not be exposed to tension. As pili exposed to force start to elongate, a larger number of pili will sequentially be stretched. Whenever a pilus is stretched and becomes exposed to force as it enters region I, the force supported by the other stretched pili is then reduced. In that way, it can be argued that the pili collectively are able to support quite large shear forces and a prerequisite for this behaviour is the strong PapG–galabiose binding. In conclusion, the PapG adhesin does not only recognise and form bonds with the host receptor. It is also important for the bacteria to maintain attachment to the uroepithelial cells, even under influence of external forces, e.g. shear forces due to the urine flow. The strong specific PapG–galabiose interaction thus contributes to a successful colonisation and invasion of the host tissue and constitutes thereby an important virulence factor.

Acknowledgments We acknowledge Prof. Bernt-Eric Uhlin and Monica Persson, Department of Molecular Biology, Umeå University, Sweden, for providing the *E. coli* strains. We thank Dr. Erik Fällman for laboratorial assistance. We also thank Prof. Ulf J. Nilsson, Organic and Bioorganic Chemistry, Lund University, Sweden for providing the amino-galabiose coated beads. Economical support from the Magn. Bergvalls Foundation, Sweden, is also acknowledged.

References

Andersson M, Fällman E, Uhlin BE, Axner O (2006a) Dynamic force spectroscopy of the unfolding of P pili. Biophys J 91:2717–2725. doi:10.1529/biophysj.106.087429

Andersson M, Fällman E, Uhlin BE, Axner O (2006b) Force measuring optical tweezers system for long time measurements of Pili stability. SPIE 6088:286–295

Andersson M, Fällman E, Uhlin BE, Axner O (2006c) A sticky chain model of the elongation of *Escherichia coli* P pili under strain. Biophys J 90:1521–1534. doi:10.1529/biophysj.105.074674

Andersson M, Uhlin BE, Fallman E (2007) The biomechanical properties of *E. coli* Pili for urinary tract attachment reflect the host environment. Biophys J 93:3008–3014. doi:10.1529/biophysj.107.110643

Barsegov V, Thirumalai D (2005) Dynamics of unbinding of cell adhesion molecules: transition from catch to slip bonds. Proc Natl Acad Sci USA 102:1835–1839. doi:10.1073/pnas.0406938102

Bell MG (1978) Models for the specific adhesion of cells to cells. Science 200:618–627. doi:10.1126/science.347575

Björnham O, Axner O, Andersson M (2008) Modeling of the elongation and retraction of *Escherichia coli* P pili under strain by Monte Carlo simulations. Eur Biophys J Biophys Lett 37:381–391

Dembo M, Torney DC, Saxman K, Hammer D (1988) The reaction-limited kinetics of membrane-to-surface adhesion and detachment. Proc R Soc Lond B Biol Sci 234:55–83

Enami M, Nakasone N, Honma Y, Kakinohana S, Kudaka J, Iwanaga M (1999) Expression of type I pili is abolished in verotoxin-producing *Escherichia coli* O157. FEMS Microbiol Lett 179:467–472. doi:10.1111/j.1574-6968.1999.tb08764.x

Evans E (2001) Probing the relation between force—lifetime—and chemistry in single molecular bonds. Annu Rev Biophys Biomol Struct 30:105–128. doi:10.1146/annurev.biophys.30.1.105

Evans E, Ritchie K (1997) Dynamic strength of molecular adhesion bonds. Biophys J 72:1541–1555

Evans E, Leung A, Hammer D, Simon S (2001) Chemically distinct transition states govern rapid dissociation of single L-selectin bonds under force. Proc Natl Acad Sci USA 98:3784–3789. doi:10.1073/pnas.061324998

Evans E, Leung A, Heinrich V, Zhu CCh (2004) Mechanical switching and coupling between two dissociation pathways in a P-selectin adhesion bond. Proc Natl Acad Sci USA 101:11281–11286

Fällman E, Schedin S, Jass J, Andersson M, Uhlin BE, Axner O (2004) Optical tweezers based force measurement system for quantitating binding interactions: system design and application for the study of bacterial adhesion. Biosens Bioelectron 19:1429–1437. doi:10.1016/j.bios.2003.12.029

Forero M, Thomas WE, Bland C, Nilsson LM, Sokurenko EV, Vogel V (2004) A catch-bond based nanoadhesive sensitive to shear stress. Nano Lett 4:1593–1597. doi:10.1021/nl049329z

Foxman B, Brown P (2003) Epidemiology of urinary tract infections—transmission and risk factors, incidence, and costs. Infect Dis Clin North Am 17:227–241. doi:10.1016/S0891-5520(03)00005-9

Fritz J, Katopodis AG, Kolbinger F, Anselmetti D (1998) Force-mediated kinetics of single P-selectin ligand complexes observed

by atomic force microscopy. Proc Natl Acad Sci USA 95:12283–12288. doi:10.1073/pnas.95.21.12283

Goldman AJ, Cox RG, Brenner H (1967) Slow viscous motion of a sphere parallel to a plane wall. II. Couette flow. Chem Eng Sci 22:653–660. doi:10.1016/0009-2509(67)80048-4

Guo B, Guilford WH (2006) Mechanics of actomyosin bonds in different nucleotide states are tuned to muscle contraction. Proc Natl Acad Sci USA 103:9844–9849. doi:10.1073/pnas.0601255103

Jass J, Schedin S, Fällman E, Ohlsson J, Nilsson U, Uhlin BE, Axner O (2004) Physical properties of *Escherichia coli* P pili measured by optical tweezers. Biophys J 87:4271–4283. doi:10.1529/biophysj.104.044867

Larsson A, Ohlsson J, Dodson KW, Hultgren SJ, Nilsson U, Kihlberg J (2003) Quantitative studies of the binding of the class II PapG adhesin from uropathogenic *Escherichia coli* to oligosaccharides. Bioorg Med Chem 11:2255–2261. doi:10.1016/S0968-0896(03)00114-7

Liang MN, Smith SP, Metallo SJ, Choi IS, Prentiss M, Whitesides GM (2000) Measuring the forces involved in polyvalent adhesion of uropathogenic *Escherichia coli* to mannose-presenting surfaces. Proc Natl Acad Sci USA 97:13092–13096. doi:10.1073/pnas.230451697

Lindberg FP, Lund B, Normark S (1984) Genes of pyelonephritogenic *E. coli* required for digalactosidespecific agglutination of human cells. EMBO J 3:1167–1173

Lindberg F, Lund B, Johansson L, Normark S (1987) Localization of the receptor-binding protein adhesin at the tip of the bacterial pilus. Nature 328:84–87. doi:10.1038/328084a0

Lugmaier RA, Schedin S, Kuhner F, Benoit M (2007) Dynamic restacking of *Escherichia Coli* P-pili. Eur Biophys J 37:111–120. doi:10.1007/s00249-007-0183-x

Lund B, Lindberg F, Marklund BI, Normark S (1987) The PapG protein is the alpha-D-galactopyranosyl-(1–4)-beta-D-galactopyranose-binding adhesin of uropathogenic *Escherichia Coli*. Proc Natl Acad Sci USA 84:5898–5902. doi:10.1073/pnas.84.16.5898

Maier B, Potter L, So M, Seifert HS, Sheetz MP (2002) Single pilus motor forces exceed 100 pN. Proc Natl Acad Sci USA 99:16012–16017. doi:10.1073/pnas.242523299

Marshall BT, Long M, Piper JW, Yago T, McEver RP, Zhu C (2003) Direct observation of catch bonds involving cell-adhesion molecules. Nature 423:190–193. doi:10.1038/nature01605

Miller E, Garcia TI, Hultgren S, Oberhauser A (2006) The mechanical properties of *E. coli* type 1 pili measured by atomic force microscopy techniques. Biophys J 91:3848–3856. doi:10.1529/biophysj.106.088989

Morfill J, Blank K, Zahnd C, Luginbuhl B, Kuhner F, Gottschalk KE, Pluckthun A, Gaub HE (2007) Affinity-matured recombinant antibody fragments analyzed by single-molecule force spectroscopy. Biophys J 93:3583–3590. doi:10.1529/biophysj.107.112532

Nilsson LM, Thomas WE, Trintchina E, Vogel V, Sokurenko EV (2006) Catch bond-mediated adhesion without a shear threshold—Trimannose versus monomannose interactions with the FimH adhesin of *Escherichia coli*. J Biol Chem 281:16656–16663. doi:10.1074/jbc.M511496200

Odorico M, Teulon JM, Bessou T, Vidaud C, Bellanger L, Chen SWW, Quemeneur E, Parot P, Pellequer JL (2007) Energy landscape of chelated uranyl: antibody interactions by dynamic force spectroscopy. Biophys J 93:645–654. doi:10.1529/biophysj.106.098129

Ohlsson J, Jass J, Uhlin BE, Kihlberg J, Nilsson UJ (2002) Discovery of potent inhibitors of PapG adhesins from uropathogenic *Escherichia coli* through synthesis and evaluation of galabiose derivatives. ChemBioChem 3:772–779. doi:10.1002/1439-7633(20020802)3:8<772::AID-CBIC772>3.0.CO;2-8

Reid G, Sobel JD (1987) Bacterial adherence in the pathogenesis of urinary-tract infection: a review. Rev Infect Dis 9:470–487

Sandberg T, Kaijser B, Lidinjanson G, Lincoln K, Orskov F, Orskov I, Stokland E, Svanborgeden C (1988) Virulence of *Escherichia Coli* in relation to host factors in women with symptomatic urinary-tract infection. J Clin Microbiol 26:1471–1476

Stromberg N, Marklund BI, Lund B, Ilver D, Hamers A, Gaastra W, Karlsson KA, Normark S (1990) Host-specificity of uropathogenic *Escherichia Coli* depends on differences in binding specificity to gal-alpha 1–4gal-containing isoreceptors. EMBO J 9:2001–2010

Sundararaj S, Guo A, Habibi-Nazhad B, Rouani M, Stothard P, Ellison M, Wishart DS (2004) The CyberCell Database (CCDB): a comprehensive, self-updating, relational database to coordinate and facilitate in silico modeling of *Escherichia coli*. Nucleic Acids Res 32:D293–D295. doi:10.1093/nar/gkh108

Thomas WE, Trintchina E, Forero M, Vogel V, Sokurenko EV (2002) Bacterial adhesion to target cells enhanced by shear force. Cell 109:913–923. doi:10.1016/S0092-8674(02)00796-1

Thomas WE, Nilsson LM, Forero M, Sokurenko EV, Vogel V (2004) Shear-dependent 'stick-and-roll' adhesion of type 1 fimbriated *Escherichia coli*. Mol Microbiol 53:1545–1557. doi:10.1111/j.1365-2958.2004.04226.x

Thomas W, Forero M, Yakovenko O, Nilsson L, Vicini P, Sokurenko E, Vogel V (2006) Catch-bond model derived from allostery explains force-activated bacterial adhesion. Biophys J 90:753–764. doi:10.1529/biophysj.105.066548

Weissman SJ, Chattopadhyay S, Aprikian P, Obata-Yasuoka M, Yarova-Yarovaya Y, Stapleton A, Ba-Thein W, Dykhuizen D, Johnson JR, Sokurenko EV (2006) Clonal analysis reveals high rate of structural mutations in fimbrial adhesins of extraintestinal pathogenic *Escherichia coli*. Mol Microbiol 59:975–988. doi:10.1111/j.1365-2958.2005.04985.x

Yang HY, Yu JP, Fu G, Shi XL, Xiao L, Chen YZ, Fang XH, He C (2007) Interaction between single molecules of Mac-1 and ICAM-1 in living cells: an atomic force microscopy study. Exp Cell Res 313:3497–3504. doi:10.1016/j.yexcr.2007.08.001